*Send Orders for Reprints to reprints@benthamscience.ae*

*Current Cancer Drug Targets*, 2015, 15, 000-000 

# The Anthelmintic Drug Niclosamide Inhibits the Proliferative Activity of Human Osteosarcoma Cells by Targeting Multiple Signal Pathways

Zhan Liao, Guoxin Nan, Zhengjian Yan, Liyi Zeng, Youlin Deng, Jixing Ye, Zhonglin Zhang, Min Qiao, Ruifang Li, Sahitya Denduluri, Jing Wang, Qiang Wei, Nisha Geng, Lianggong Zhao, Shun Lu, Xin Wang, Guolin Zhou, Hue H. Luu, Rex C. Haydon, Tong-Chuan He* and Zhongliang Wang

*The University of Chicago Medical Center*

**T.C. He**

**Abstract:** Osteosarcoma (OS) is the most common primary malignant tumor of bone with a high propensity for lung metastasis. Despite significant advances in surgical techniques and chemotherapeutic regimens over the past few decades, there has been minimal improvement in OS patient survival. There is an urgent need to identify novel antitumor agents to treat human OS. Repurposing the clinically-used drugs represents a rapid and effective approach to the development of new anticancer agents. The anthelmintic drug niclosamide has recently been identified as a potential anticancer agent in human cancers. Here, we investigate if niclosamide can be developed as an anti-OS drug. We find that niclosamide can effectively inhibit OS cell proliferation and survival at low micromolar concentrations. Cell migration and wounding closure are significantly inhibited by niclosamide. Niclosamide induces cell apoptosis and inhibits cell cycle progression in OS cells. Analysis of niclosamide's effect on 11 cancer-related signal pathway reporters reveals that three of them, the E2F1, AP1, and c-Myc-responsive reporters, are significantly inhibited. To a lesser extent, the HIF1α, TCF/LEF, CREB, NFκB, Smad/TGFβ, and Rbpj/Notch pathway reporters are also inhibited, while the NFAT and Wnt/β-catenin reporters are not significantly affected by niclosamide treatment. We demonstrate that the expression of c-Fos, c-Jun. E2F1, and c-Myc in OS cells is effectively inhibited by niclosamide. Furthermore, niclosamide is shown to effectively inhibit tumor growth in a mouse xenograft tumor model of human osteosarcoma cells. Taken together, these results strongly suggest that niclosamide may exert its anticancer activity in OS cells by targeting multiple signaling pathways. Future investigations should be directed to exploring the antitumor activity in clinically relevant OS models and ultimately in clinical trials.

**Keywords:** Anticancer agent, bone tumors, drug repurposing, niclosamide, osteosarcoma, sarcomas.

## INTRODUCTION

Osteosarcoma (OS) is the most common non-hematological malignant tumor of bone in children and adults, with its peak incidence in the teens [1-5]. OS usually involves the metaphysis of long bones where high bone turnover occurs during longitudinal growth spurts [6]. OS is characterized by a high propensity for lung metastasis with 10%-20% having detectable metastases at diagnosis [7]. These pulmonary lesions are responsible for the high mortality associated with OS [4, 6]. Only about 15-20% of patients have radiographically detectable pulmonary metastases, while approximately 80% of the patients either will develop or already have radiographically undetectable micrometastases [4-6, 8]. Although the pathogenesis underlying OS is poorly understood, the tumors often develop in settings of high bone turnover, such as the adolescent growth spurt [4-6, 9]. Numerous genetic and cytogenetic abnormalities have been associated with OS, including mutations of tumor suppressors and oncogenes, as well as chromosomal amplifications, deletions, rearrangements, and translocations [1, 3-6, 9, 10]. We have demonstrated that Wnt/β-catenin, IGF signaling, S100A6 and lysophosphatidic acid acyltransferase β (LPAATβ) are up-regulated in human OS tumors [10-18]. Increasing evidence suggests that disruptions of osteogenic differentiation may lead to OS development as osteogenic BMPs can promote osteosarcoma growth [3, 4, 19-23].

The clinical management of OS includes surgical resection of both primary and/or pulmonary lesions combined with pre- and post-operative chemotherapy [4, 6, 8]. Without systemic treatment, few OS patients achieve long-term disease-free status, even with optimal local treatment [9]. Once a metastasis has been detected, the disease is likely to relapse. Thus, clinical management of OS faces numerous challenges, including adverse effects associated with chemotherapies, chemoresistance, recurrence, and pulmonary metastasis [2-4]. Recent studies indicate that differentiation therapy may represent an attractive alternative and/or adjuvant therapy to conventional chemotherapy [24-28]. We and other demonstrated that some agonists of nuclear receptors can inhibit proliferation and promote differentiation in cancer cells, including OS cells [26, 28-34].

*Address correspondence to Zhongliang Wang of Chongqing Medical University, Tel: (011)-86-23-63622045; E-mail: 4829855@163.com; or T.-C. He of The University of Chicago Medical Center, Tel: (773) 702-7169; Fax: (773) 834-4598; E-mail: tche@uchicago.edu

1568-0096/15 $58.00+.00 

Repurposing the clinically-used drugs represents a rapid and effective approach to the discovery and development of new anticancer agents. For the past five years, niclosamide has been repeatedly identified as as a potential anticancer agent by various high-throughput screening campaigns [35]. Niclosamide (trade name Niclocide) is a teniacide in the anthelmintic family, especially effective against cestodes that infect humans, and has been approved for use in humans for nearly 50 years. Niclosamide was thought to inhibit oxidative phosphorylation and stimulates adenosine triphosphatase activity in the mitochondria of cestodes (e.g. tapeworm), killing the scolex and proximal segments of the tapeworm both *in vitro* and/or *in vivo*, which is well tolerated in humans [35]. Several studies have shown that niclosamide exhibits effective anticancer activity and inhibits the growth of colon rectal cancer [36-38], lung cancer [39, 40], breast cancer [41-44], ovarian cancer [45-47], prostate cancer [41, 48], glioblastoma [49], head and neck cancer [50], leukemia [51, 52], and human uterine leiomyoma [53]. Despite significant advances in surgical techniques and chemotherapeutic regimens over the past few decades, there has been minimal improvement in patient survival. Thus, there is an urgent need to identify novel and more effective antitumor agents to treat human OS.

In this report, we investigate if niclosamide inhibits the proliferation of human OS cells. Using the commonly used OS cell lines, we find that niclosamide can effectively inhibit OS cell proliferation and survival at low micromolar concentrations. Cell migration and wounding closure are also significantly inhibited by niclosamide at very low concentrations. Niclosamide is capable of inducing cell apoptosis and inhibits cell cycle progression in OS cells. To explore possible molecular mechanism underlying niclosamide's anti-proliferative activity we analyze niclosamide's effect on 11 cancer-related signal pathway reporters and find that three of the tested 11 pathway reporters, E2F1, AP1, and c-Myc-responsive reporters, are significantly inhibited at as early as 24h after niclosamide treatment. The E2F1 and AP1 reporters are even more pronouncedly inhibited at 48h post treatment. We find that HIF1α, TCF/LEF, CREB, NFκB, Smad/TGFβ, and Rbpj/Notch pathway reporters are also inhibited, to a lesser extent, while the NFAT reporter is not significantly affected by niclosamide treatment. Interestingly, contrary to the prior reports [36, 37, 41, 46, 47, 53, 54], the Wnt signal pathway TCF/LEF reporter activity is not significantly inhibited in OS cells. We further demonstrate that the expression of c-Fos and c-Jun (the AP1 pathway), E2F1, and c-Myc in OS cells is effectively inhibited at as low as 0.25μM niclosamide. Furthermore, niclosamide is shown to effectively inhibit xenograft tumor growth in a mouse model of human osteosarcoma cells. Taken together, these results strongly suggest that niclosamide may exert its anticancer activity by targeting multiple signaling pathways.

## MATERIALS AND METHODS

### Cell Culture and Chemicals

Human osteosarcoma lines MG63 and 143B were purchased from ATCC (Manassas, VA) and maintained in complete Dulbecco's Modified Eagle's Medium (DMEM) containing 10% fetal bovine serum (FBS, Invitrogen, Carlsbad, CA), 100 units of penicillin and 100μg of streptomycin at 37°C in 5% $CO_2$ [55-61]. Niclosamide was purchased from Cayman Chemical (Ann Arbor, MI). Unless indicated otherwise, all chemicals were purchased from Sigma-Aldrich (St. Louis, MO) or Fisher Scientific (Pittsburgh, PA).

### Crystal Violet Viability Assay

Crystal violet assay was conducted as described [11, 13, 15, 17, 19, 55, 56, 61-65]. Briefly, subconfluent osteosarcoma cells were treated with varied concentrations of niclosamide or DMSO control. At 48h or 72h after treatment, cells were carefully washed with PBS and stained with 0.5% crystal violet/formalin solution at room temperature for 20-30 min. The stained cells were washed with tape water and air dried for taking macrographic images [57]. For quantitative measurement, the stained cells were dissolved in 10% acetic acid (1 ml per well for 12-well plate) at room temperature for 20 min with shaking. 500μl were taken and added to 2 ml $ddH_2O$. Absorbance at 570-590nm was measured [56, 57, 66].

### Apoptosis Analysis with Hoechst 33258

Exponentially growing 143B and MG63 cells were treated with 1.5μM and 3.0μM niclosamide or DMSO control. At 48h post treatment, cells were collected, fixed and stained with the Magic Solution (0.5% NP-40, 3.4% formaldehyde and 10μg/ml Hoechst 33258, in PBS). Apoptotic cells were observed and recorded under a fluorescence microscope. Each assay condition was done in triplicate; and the results were repeated at least in three independent batches of experiments. The average numbers of apoptotic cells were calculated by counting apparent apoptotic cells in at least ten 100x magnification images for each assay condition.

### Apoptosis Analysis Using Annexin V-FITC Flow Cytometry

The annexin V staining apoptosis assay was performed as previously described [60, 66, 67]. Briefly, exponentially growing 143B and MG63 cells were seeded in 6-well plates and treated with niclosamide (10μM) or DMSO control. At 24h post treatment, cells were trypsinized, washed with PBS, resuspended in Annexin V Binding Buffer at a density of $10^6$ cells/ml, and stained with Annexin V-FITC (BD Pharmingen, San Jose, CA) and propidium iodide for 15min at room temperature under a light-proof condition. The stained cells were subjected to flow cytometry analysis using the BD FACSCalibur-HTS. The acquired flow cytometry data were analyzed by using the FlowJo v10.0 software. Each assay condition was done in triplicate.

### Cell Scratching/Wounding Assay

Cell wound healing migration assays were performed as previously described [34, 60, 68]. Briefly, exponentially growing cells were seeded in 6-well cell culture plates at subconfluency. Once the cells reached approximately 90% confluence, the monolayer cells were wounded with pipette tips. At various time points after wounding, the wound

healing at the approximately same fields was recorded under bright field microscopy. These assays were done in triplicate. The average gap widths were measured and determined from at least ten low-power field images for each assay condition using Olympus Cellsens Digital Imaging software. The percentage of gap remaining open was calculated by dividing the average gap width at a given time point with the respective average gap width at 0h.

### Flow Cytometry Analysis

Subconfluent 143B and MG63 cells were seeded in 6-well plates and treated with 1.0μM niclosamide or DMSO for 24h or 48h. The treated cells were harvested, fixed and stained with the Magic Solution (10x stock: 0.5% NP-40, 3.4% formaldehyde, 10μg/ml Hoechst 33258, in PBS) at room temperature for 5-10min, and washed twice with PBS on ice. The stained cells were subjected to flow cytometry analysis using the bench-top cell analyzer BD FACSCalibur-HTS. Each assay condition was done in triplicate. Acquired flow cytometry data were further analyzed with the FlowJo v10.0 software.

### Cell Transfection and Gaussia Luciferase Reporter Assay

Gaussia luciferase reporter assay was carried out as described previously [59, 68-71]. The tested 11 cancer-relate signaling pathway reporters, including HIF1α, TCF1/Lef1, E2F, AP1, NFκB, c-Myc, CREB, NFAT, TGFβ/Smad, STAT, and Rbpj reporters [72]. Briefly, 143B cells were seeded in 25 $cm^2$ culture flasks and transfected with 3.0μg per flask of the 11 cancer-related signal pathway reporter plasmids as previously described [72] using LipofectAMINE (Invitrogen). At 16h post transfection, cells were replated in 12-well plates and treated with various concentrations of niclosamide or DMSO solvent control. At 24h and 48h post treatment, cells were lysed and subjected to Gaussia luciferase activity assays BioLux Gaussia Luciferase Assay Kit (New England Biolabs). Each assay condition was done in triplicate. Luciferase activity was normalized by total cellular protein concentrations among the samples.

### RNA Isolation and Quantitative Real-Time PCR (qPCR)

Subconfluent 143B cells were treated with varied concentrations of niclosamide for 48h. Total RNA was isolated from the treated cells by using TRIZOL Reagents (Invitrogen) and subjected to generate cDNA templates by reverse transcription reactions with hexamer and M-MuLV reverse transcriptase (New England Biolabs, Ipswich, MA). The cDNA products were used as PCR templates. PCR primers were designed by using the Primer3 program and used to amplify the genes of interest (approximately 150-250bp). The primers used for qPCR include the following: human c-Fos, forward 5'-AGA ATC CGA AGG GAA AGG AA-3' and reverse 5'-CTT CTC CTT CAG CAG GTT GG-3'; human c-Jun, forward 5'-CAG GTG GCA CAG CTT AAA CA-3' and reverse 5'-TTT TTC TCT CCG TCG CAA CT-3'; human E2F1, forward 5'-ATG TTT TCC TGT GCC CTG AG-3' and reverse 5'-ATC TGT GGT GAG GGA TGA GG-3'; human c-Myc, forward 5'- CGT CCT GGG AAG GGA GAT-3' and reverse 5'- CGC TGC TAT GGG CAA AGT-3'; and human GAPDH, forward 5'-ATG TTT TCC TGT GCC CTG AG-3' and reverse 5'- ATC TGT GGT GAG GGA TGA GG-3'. The qPCR were carried out as described [17, 21, 56-58, 60, 69, 71, 73-81]. Briefly, the SYBR Green-based qPCR analysis was carried out by using the thermocycler Opticon II DNA Engine (Bio-Rad, CA) with a standard pUC19 plasmid. The qPCR reactions were done in triplicate. PCR products were resolved on 1.5% agarose gels. All samples were normalized by the expression level of GAPDH.

### Xenograft Tumors of Human Osteosarcoma Cancer Cells

The use and care of animals were approved by the Institutional Animal Care and Use Committee. 143B stably labeled with firefly luciferase (143B-Fluc) was constructed with *piggyBac* transposon system [56, 58, 61]. Exponentially growing 143B-Fluc cells were collected, resuspended at $10^7$ cells/ml and injected periosteally around tibia of the athymic nude mice (Harlan Laboratories, 6-8 week old, female, $10^6$ cells per injection). At 3 days after cancer cell injection, the mice were divided into two groups (n=6 per group), and treated with niclosamide at 10mg/kg or DMSO intra-peritoneally once every two days. The growth of tumors were monitored by whole body bioluminescence imaging using the Xenogen IVIS 200 Imaging System at days 4, 11, and 18 after drug treatment. The mice were sacrificed at the end of week 3 after. The average signal for each group at different time points were calculated using the Xenogen's Living Image analysis software as reported [17, 19, 60].

### Statistical Analysis

The quantitative assays were performed in triplicate and/or repeated three times. Data were expressed as mean ± SD. Statistical significances were determined by one-way analysis of variance and the student's *t* test. A value of $p<0.05$ was considered statistically significant.

## RESULTS AND DISCUSSION

### Niclosamide Inhibits the Proliferation and Survival of Human Osteosarcoma Cells

To test if niclosamide can be used as a potentially repurposed anticancer agent for osteosarcoma, we tested if niclosamide can effectively inhibit the proliferation and survival of two commonly-used human osteosarcoma cell lines, 143B and MG63. 143B is one of the most aggressive osteosarcoma lines and can effectively develop lung metastasis in orthotopic animal models [17, 62, 65]. We found that 143B cell proliferation was noticeably inhibited at 4μM at 48h and became more apparent at 0.5μM at 72h (Fig. **1A**, panel **a**). Quantitative analysis indicates that the cell survival rates decreased significantly at 72h in a dose-dependent fashion and were 35.8%, 27.1%, 18.3%, 11.8%, and 9.8% of the DMSO control's at 0.5μM, 1.0μM, 2.0μM, 4.0μM and 8.0μM niclosamide, respectively ($p<0.001$) (Fig. **1A**, panel **b**). MG63 cells are known to be less aggressive, but their proliferation was effectively inhibited at 0.5μM niclosamide both at 48h and 72h although there was a significantly dose-dependent effect (Fig. **1B**, panel **a**). In fact, the cell survival rates were 46.4%, 33.5%, 22.9%, and 16.4% of the DMSO control group's at 0.5μM, 1.0μM,

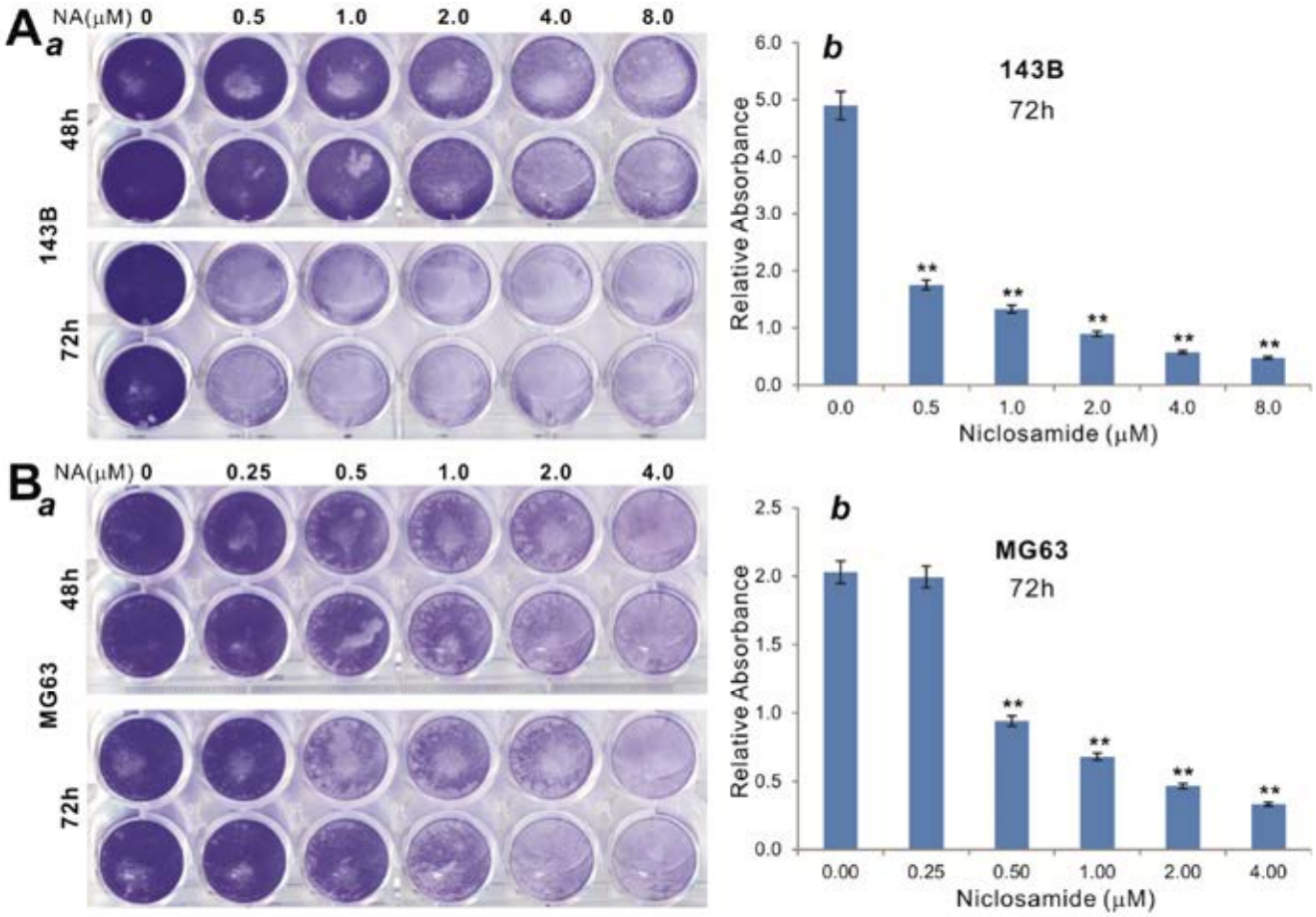


**Fig. (1). Niclosamide inhibits the proliferation and survival of human osteosarcoma cells**. Exponentially growing 143B (**A**) and MG63 (**B**) cells were seeded in 24-well cell culture plates and treated with the indicated concentrations of niclosamide for 48h and 72h. The viable cells were fixed and stained with Crystal violet (***a***). For quantitative determination, the stained cells for the 72h time point were dissolved in acetic acid and subjected to absorbance reading at 570-590nm (***b***). Each assay condition was done in triplicate; and the results were repeated at least in three independent batches of experiments. Representative results are shown. "**", *p<0.001* (compared with the control group).

2.0μM, and 4.0μM niclosamide, respectively ($p$<0.001) (Fig. **1B**, panel **b**). The anti-proliferative activity of niclosamide was also found in several other OS cell lines, such as TE-85, HOS/MNNG, U2OS and SaOS2 cell lines, and the OS patient-derived OS lines established in our lab [13, 19] (data not shown). Therefore, these results strongly suggest that niclosamide may effectively inhibit osteosarcoma cell proliferation.

### Niclosamide Inhibits the Cell Migration and Wounding Closure of Human Osteosarcoma Cells

We further examined the effect of niclosamide on cell migration after monolayer wounding. When monolayer 143B cells were wounded and treated with 1.5μM and 3.0μM niclosamide, the niclosamide-treated groups closed the gaps at much slower pace at 12h and 20h time points, compared with that of the DMSO control group (Fig. **2A**, panel **a**). In fact, the open gaps in the niclosamide treatment groups remained 62.1% and 61.5% at 12h, and 45.9% and 53.3% of the original gaps (at 0h) at 20h for 1.5μM and 3.0μM niclosamide, respectively ($p$<0.001) (Fig. **2B**, panel **a**). Similar results were obtained in MG63 cells except that the niclosamide exhibited even strongly inhibitory effects (Fig. **2A**, panel **a**). Quantitatively, at the 20h time point the percentages of gap remaining open were 42.3%, 49.4%, and 84.2% for DMSO, 1.5μM and 3.0μM niclosamide groups, respectively, although only the difference between the 3.0μM niclosamide group and DMSO group was statistically significant ($p$<0.001) (Fig. **2A**, panel **b**). However, at the 43h time point both niclosamide treatment groups exhibited significantly gaps, compared with the DMSO control group ($p$<0.001) (Fig. **2A**, panel **b**). Taken together, our results indicate that niclosamide can effectively inhibit osteosarcoma cell migration.

### Niclosamide Effectively Induces Apoptosis and Inhibits Cell Cycle Progression of Human Osteosarcoma Cells

To investigate possible mechanisms underlying niclosamide's anti-proliferative activity, we tested if niclosamide can induce apoptosis in osteosarcoma cells. When 143B and MG63 cells were treated with 1.5μM and 3.0μM niclosamide or DMSO control, apoptotic cells were readily detected in the niclosamide-treated cells, compared with those treated by DMSO (Fig. **3A**). Cells treated with 3.0μM niclosamide exhibited slightly higher numbers of apoptotic cells than that treated with 1.5μM niclosamide.

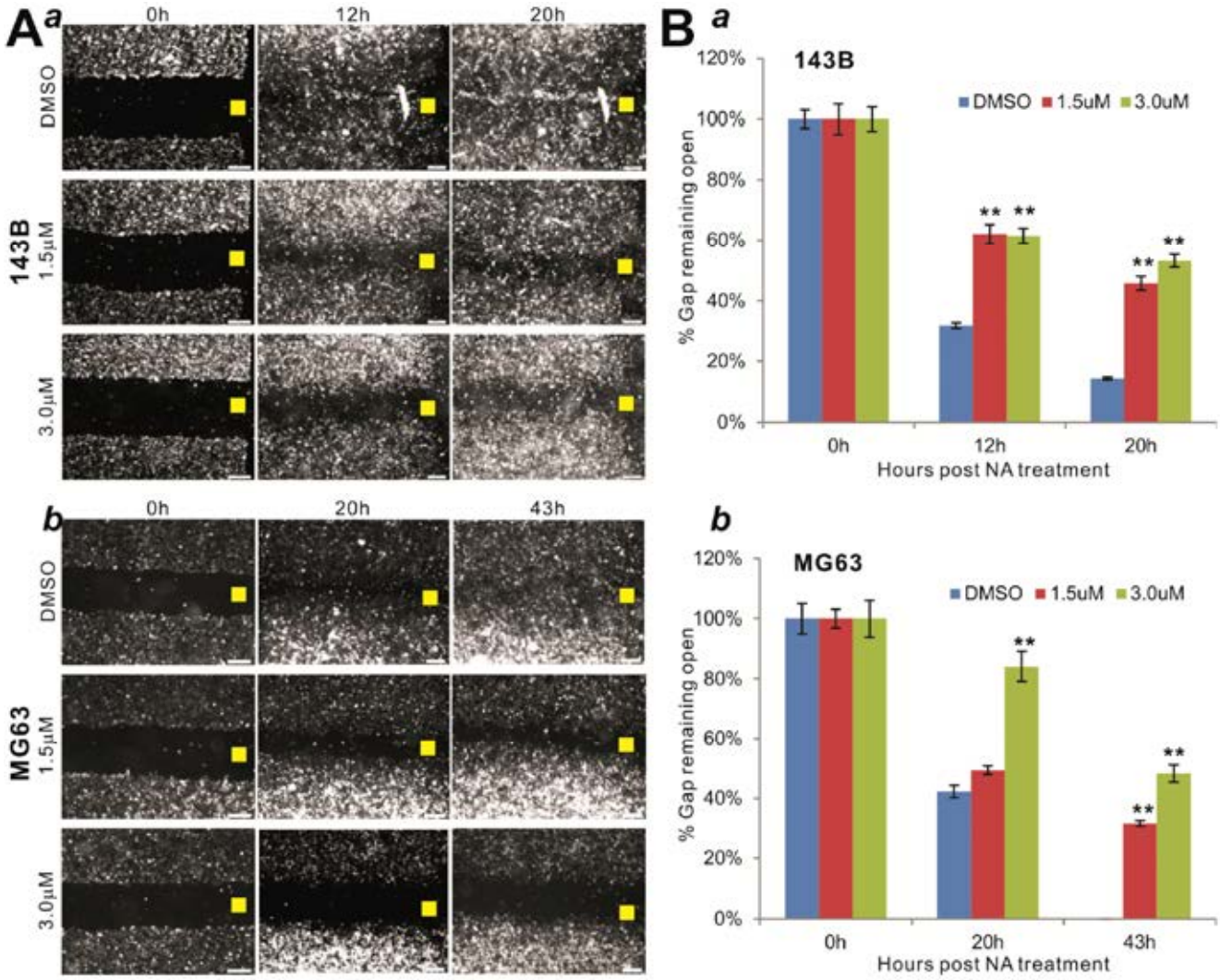


**Fig. (2). Niclosamide inhibits the cell migration and wounding closure of human osteosarcoma cells**. (**A**) Exponentially growing 143B (***a***) and MG63 (***b***) cells were seeded in 6-well cell culture plates. Once cells reached confluence, cell wounding was created with pipet tips and then treated with 1.0μM niclosamide or DMSO control. The wound closure status was monitored and recorded at the indicated time points. Each assay condition was done in triplicate; and the results were repeated at least in three independent batches of experiments. (**B**) Quantitative analysis of wound closure in 143B (***a***) and MG63 (***b***) cells. The average gap widths were measured and determined from at least ten low-power field images for each assay condition using Olympus Cellsens Digital Imaging software. The percentage of gap remaining open was calculated by dividing the average gap width at a given time point with the respective average gap width at 0h. "**", *p<0.001* (compared with the control group). The yellow squares indicate the reference points for microphotographing. Representative results are shown.

Quantitative analysis indicates that niclosamide induced 4.4 and 6.3 times higher in numbers of apoptotic cells in 143B cells than DMSO control groups at 1.5μM and 3.0μM niclosamide, respectively ($p$<0.001) (Fig. **3B**). In MG63 cells, 1.5μM and 3.0μM niclosamide treatment induced 3.3 and 4.5 times of apoptotic cells compared with that in the DMSO control groups ($p$<0.001) (Fig. **3B**). We further analyzed niclosamide-induced apoptosis by using the annexin V-FITC labeling assay. We found that niclosamide treatment led to a significant increase in the percentage of apoptotic cells (Fig. **3C**). Specifically, niclosamide treatment (at 10μM) caused 43.6% and 40.0% apoptotic cells in 143B and MG63 cells, respectively, while the basal apoptotic cells were at 6.3% and 5.2% for 143B and MG63 cells (Fig. **3D**). Taken together, these findings suggest that niclosamide-induced apoptosis may be at least in part responsible for niclosamide's anti-proliferative activity in osteosarcoma cells.

We further investigated if niclosamide impacted the cell cycle progression of the treated osteosarcoma cells. When the 143B cells were treated with 1.0μM niclosamide or DMSO and subjected to cell cycle profile analyses, we found that at 24h post treatment the percentage of the G1 phase in the niclosamide-treated 143B cells increased while the S and G2 phases decreased, compared with that in the DMSO control group (Fig. **4A**, panels **a** *vs.* **b**). Statistical analysis indicated that niclosamide treatment led to a significantly increased G1 phase ($p$<0.001), decreased S phase ($p$<0.05), and reduced G2 phases ($p$<0.001) (Fig. **4A**, panel **c**). Similar results were obtained from MG63 cells. Specifically, at 48h

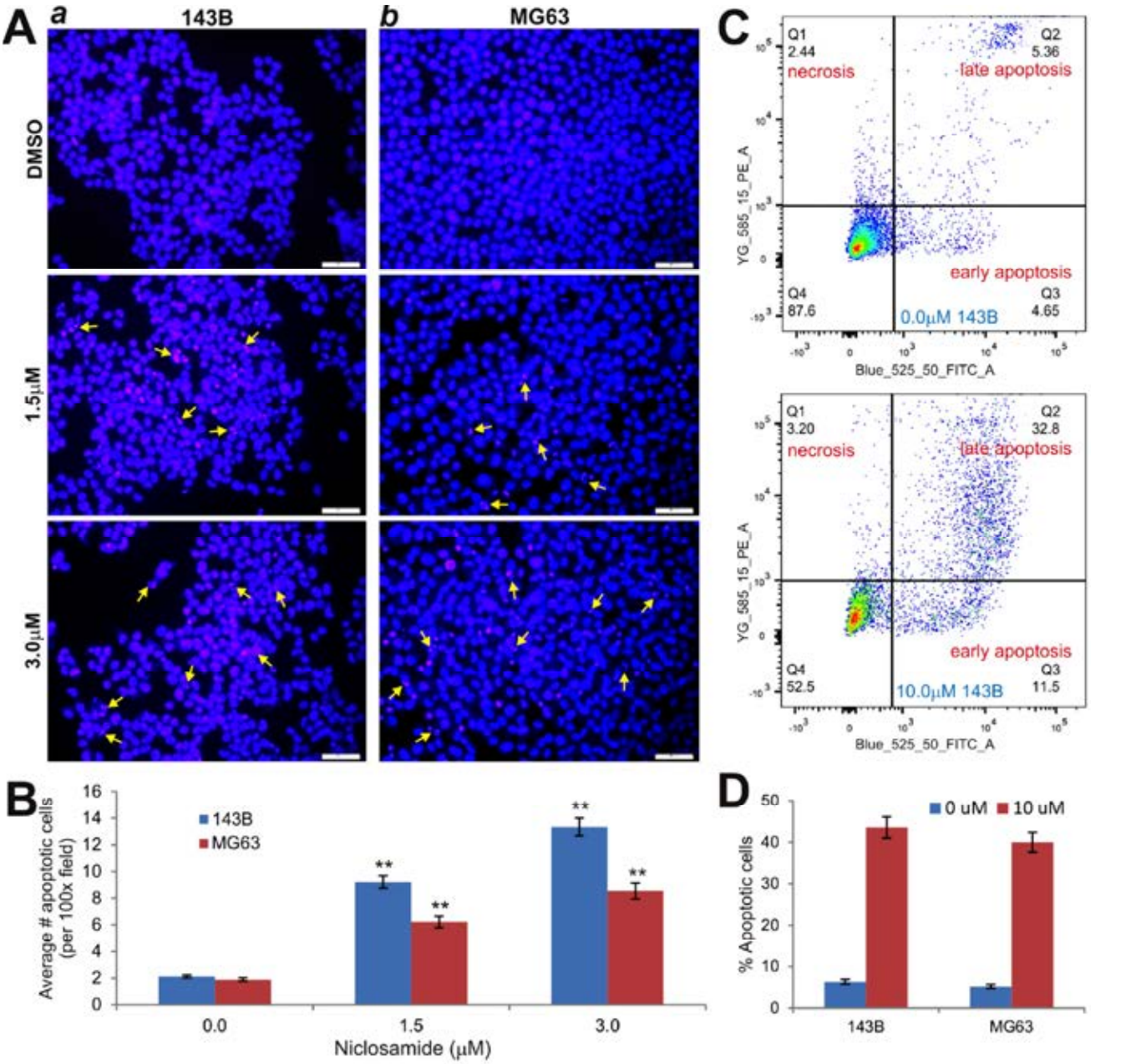


**Fig. (3). Niclosamide effectively induces apoptosis of human osteosarcoma cells**. (**A**) Exponentially growing 143B (***a***) and MG63 (***b***) cells were treated with 1.5μM and 3.0μM niclosamide or DMSO control. At 48h post treatment, cells were collected, fixed and stained with Hoechst 33258. Apoptotic cells (indicated by yellow arrows) were observed and recorded under a fluorescence microscope. Each assay condition was done in triplicate; and the results were repeated at least in three independent batches of experiments. Representative results are shown. (**B**) Quantitative analysis of average numbers of apoptotic cells. The average numbers of apoptotic cells were calculated by counting apparent apoptotic cells in at least ten 100x magnification images for each assay condition. "**", $p<0.001$ (compared with the control group). (**C**) and (**D**) Annexin-V apoptosis analysis. Exponentially growing 143B and MG63 cells were treated with niclosamide (10μM) or DMSO control. At 24h post treatment, cells were trypsinized, washed with PBS, resuspended in Annexin V Binding Buffer and stained with Annexin V-FITC (BD Pharmingen) and propidium iodide. The stained cells were subjected to flow cytometry analysis. Representative results from 143B cells are shown (**C**). The acquired flow cytometry data were analyzed by using the FlowJo v10.0 software and % apoptotic cells (including both early and late apoptosis stages) were calculated (**D**). Each assay condition was done in triplicate.

post treatment the percentage of the G1 phase in the niclosamide-treated MG63 cells increased while the S phase decreased, compared with that in the DMSO control group (Fig. **4B**, panels **a** *vs.* **b**). Further analysis indicated that niclosamide treatment led to a significantly increased G1 phase ($p<0.001$) and a significantly decreased S phase ($p<0.001$), while there was no significant change in G2 phase ($p>0.05$) (Fig. **4B**, panel **c**). Taken together, these results indicate that niclosamide exhibits its anti-proliferative activity by inducing G1 arrest and inhibiting the cell cycle progression of human osteosarcoma cells.

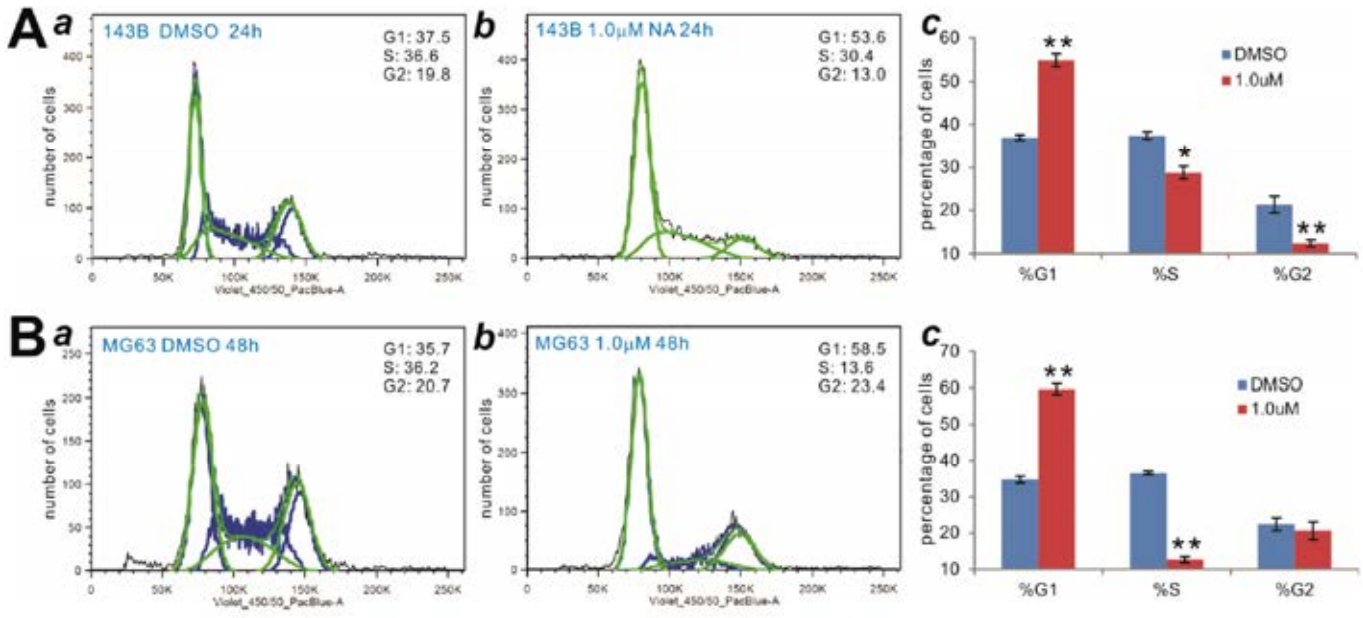


**Fig. (4). Niclosamide induces G1 arrest and inhibits the cell cycle progression of human osteosarcoma cells**. Exponentially growing 143B (**A**) and MG63 (**B**) cells were treated with 1.0μM niclosamide or DMSO control. At 24h (for 143B) or 48h (for MG63) post treatment, cells were collected, fixed and stained with Hoechst 33258, and then subjected to flow cytometry analysis using the bench-top cell analyzer BD FACSCalibur-HTS (***a*** & ***b***). Each assay condition was done in triplicate. Representative results are shown. Acquired flow cytometry data were further analyzed with the FlowJo v10.0 software. Average % of the cells in G1, S and G2 phases was graphed (***c***). "*", *p<0.05*; "**", *p<0.001* (compared with the DMSO group).

## Niclosamide Inhibits Multiple Signaling Pathways in Human Osteosarcoma Cells

The molecular basis underlying the anticancer activity of niclosamide remains largely undefined. Using the reporters of 11 cancer signaling pathways [66, 67, 72], we assessed the effect of niclosamide on this panel of reporters. When exponentially growing 143B cells were treated with 1.0μM niclosamide or DMSO for 24h and 48h, we found that three of the tested 11 pathway reporters, E2F1, AP1, and c-Myc-responsive reporters, were significantly inhibited at as early as 24h after niclosamide treatment (Fig. **5A**). The E2F1 and AP1 reporters were even more pronouncedly inhibited at 48h post treatment. We also found that the NFAT reporter was not significantly affected by niclosamide treatment, while HIF1α, TCF/LEF, CREB, NFκB, Smad/TGFβ, and Rbpj/Notch pathway reporters were only slightly inhibited at 24h (Fig. **5A**). Interestingly, contrary to the prior reports [36, 37, 41, 46, 47, 53, 54], the Wnt signal pathway TCF/LEF reporter activity was not effectively inhibited. These results were also confirmed by immunofluorescence staining of the β-catenin level, which showed that niclosamide treatment did not affect the β-catenin level in 143B cells (data not shown). Nonetheless, these results strongly suggest that niclosamide may exert its anticancer activity by targeting multiple signaling pathways.

Based on the reporter assay results, we further analyzed the effects of niclosamide on the expression levels of the three affected signaling pathways, including E2F1, c-Myc, c-Fos and c-Jun. When the exponentially growing 143B and MG63 cells were treated with the varied concentrations of niclosamide or DMSO for 48h, the isolated RNA was subjected to quantitative real-time PCR analysis using primers specific for mouse c-Fos, c-Jun, E2F1, and c-Myc. We found that the expression of c-Fos and c-Jun (the AP1 pathway) and c-Myc was effectively inhibited at as low as 0.25μM niclosamide ($p<0.001$) (Fig. **5B**). The expression of E2F1 was also significantly inhibited at 0.5μM niclosamide ($p<0.001$) (Fig. **5B**). These results further confirmed the findings from the reporter analysis shown in Fig. **5A**. Taken together, our results indicate that niclosamide may inhibit multiple signaling pathways, at least in human osteosarcomas, to exert its potent antitumor activity.

## Niclosamide Inhibits Tumor Growth in the Xenograft Model of Human Osteosarcoma Cells

In order to demonstrate the niclosamide's antitumor activity *in vivo*, we conducted *in vivo* analysis using the mouse xenograft tumor model of human osteosarcoma cells. luciferase (143B-Fluc) was constructed with *piggyBac* transposon system [56, 58, 61]. The exponentially growing 143B-Fluc cells were first periosteally injected around tibia of the athymic nude mice. At three days after injection, the mice were treated with niclosamide 10mg/kg intraperitoneally once every two days or DMSO. The tumor growth was monitored by using whole body bioluminescence imaging using the Xenogen IVIS 200 Imaging System at days 4, 11, and 18 after drug treatment (Fig. **6A**). Quantitative analysis indicated that the average signal for the niclosamide treatment group was significantly lower than that of the DMSO control group's at week 2 and week 3 time points (Fig. **6B**). These results demonstrate that niclosamide exhibits strong antitumor activity against osteosarcoma cells in the mouse xenograft model, although extensive studies in

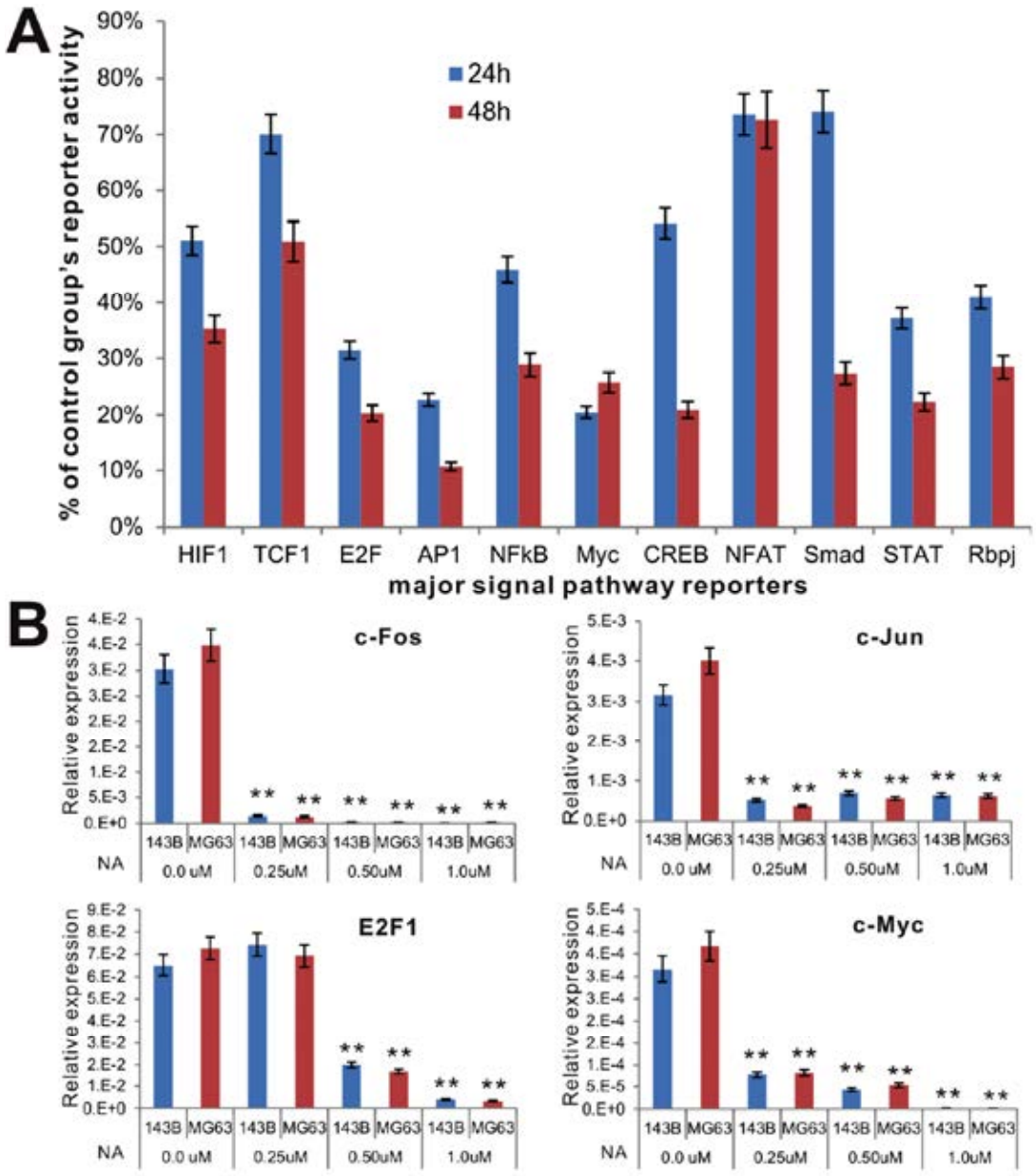


**Fig. (5). Niclosamide inhibits multiple signaling pathways in human osteosarcoma cells**. (**A**) Exponentially growing 143B cells were seeded in 24-well cell culture plates and transfected with the plasmids for the Gaussia luciferase reporters of the indicated 11 pathways, and treated with 1.0μM niclosamide or DMSO control. At 24h and 48h post treatment, culture media were collected and subjected to Gaussia luciferase assays using the BioLux Gaussia Luciferase Assay Kit (New England Biolabs). Each assay condition was done in triplicate. The % of remaining reporter activity in each treatment group was calculated by dividing the treatment group's luciferase activity with the respective DMSO group's lunciferase activity. (**B**) qPCR analysis. Exponentially growing 143B and MG63 cells were treated with the indicated concentrations of niclosamide or DMSO. At 48h post treatment, total RNA was isolated from the treated cells and subjected to qPCR analysis using primers specific for mouse c-Fos, c-Jun, E2F1, and c-Myc. All samples were normalized by endogenous GAPDH levels. Each assay condition was done in triplicate. "**", $p<0.001$ (compared with the DMSO or 0.0μM control group).

clinically-relevant osteosarcoma animal models, including the use of patient-derived xenograft model, are needed.

### The Molecular Underpinning of Niclosamide-Mediated Anticancer Activity Remains to Be Fully Elucidated

Since it was reported that niclosamide may be repurposed as an anticancer agent, several studies have been carried out to delineate its potential molecular mechanisms [35]. One of the earliest studies showed that niclosamide can inhibit Notch signaling in K562 cells [51]. A cell-based screening assay identified niclosamide as one of the candidate compounds that were capable of stimulating autophagy and inhibiting mTORC1 signaling in cells maintained in nutrient-rich conditions [82, 83]. Consistent with our pathway reporter assay results, several signaling pathways have been reported as the targets of niclosamide action. For example, niclosamide

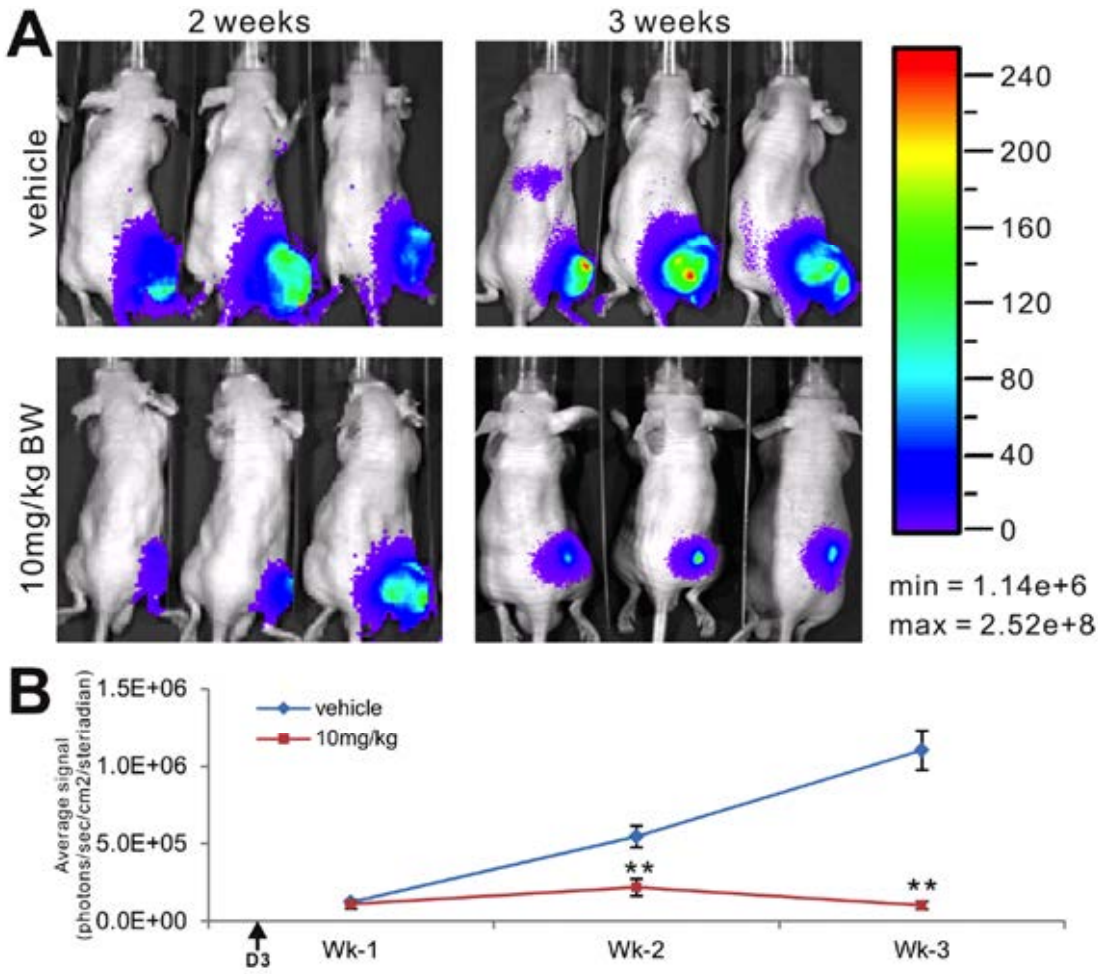


**Fig. (6). Niclodsamide inhibits the growth of xenograft tumor of human osteosarcoma cells in athymic nude mice**. **(A)** Xenogen bioluminescence imaging of xenograft tumor growth. Firefly luciferase-labeled 143B cells were injected periosteally into athymic nude mice, and treated with niclosamide (10mg/kg) or DMSO vehicle control at day 3 (indicated by an arrow), intraperitoneally once every two days. The mice were imaged at 4 (wk-1), 11 (wk-2), and 18 (wk-3) days after drug treatment. Representative images are shown. (**B**) The average signal for each group at different time points were calculated using the Xenogen's Living Image analysis software. *"**", p<0.001* (compared with the DMSO or 0.0μM control group).

was shown to inactivate NFκB pathway and generate reactive oxygen species in acute myelogenous leukemia stem cells [52]. Niclosamide inhibited the activation and transcriptional function of STAT3 and consequently induced cell growth inhibition, apoptosis, and cell cycle arrest of the cancer cells with constitutively active STAT3 [84]. A recent study suggests that niclosamide can overcome the acquired resistance to erlotinib through suppression of STAT3 in non-small cell lung cancer [39], and reversed radioresistance of human lung cancer [40]. It was reported that inhibition of STAT3 by niclosamide synergized with erlotinib against head and neck cancer [50]. S100A4-induced metastasis formation in a mouse model of colon cancer was effectively inhibited by niclosamide [38]. Several studies demonstrated that niclosamide may effectively target and inhibit the canonical Wnt/β-catenin signal pathway [36, 37, 41, 46, 47, 53, 54]. Furthermore, niclosamide was shown to induce apoptosis, impairs metastasis and reduces immunosuppressive cells in breast cancer model [43]. More recently, it was reported that niclosamide inhibited the expression of androgen receptor variants and overcame enzalutamide resistance in castration-resistant prostate cancer [48]. Niclosamide has been reported to inhibit the proliferation and/or growth of human glioblastoma [49], basal-like breast cancer [44], and the breast cancer-like stem cells [42]. While our manuscript was under review, it was reported that niclosamide induces apoptosis and cell cycle arrest *in vitro* in human OS lines [85]. Thus, our findings and the results from this report collectively demonstrate that niclosamide has strong anti-OS activity and should be further explored as potential combinatorial or adjuvant therapies for OS tumors.

Our multiple signal pathway reporter analysis indicates that niclosamide can also effectively target E2F, c-Myc and AP-1 pathways in human osteosarcoma cells. Interestingly, a recent study reported that niclosamide acted as an effective radiosensitizer in non-small cell lung cancer cells by enhancing ROS-mediated cell death through c-Jun activation, suggesting that niclosamide may be a promising radiosensitizer in lung cancer cells through activation of the p38 MAPK-c-Jun axis [86]. However, it was not clear if the AP-1 activity

was affected under this condition. It should also be pointed out that our pathway reporter analysis failed to demonstrate a significant inhibition of the Wnt signal pathway by niclosamide, which is in contrast to several prior reports [36, 37, 41, 46, 47, 53, 54]. While we do not have any satisfactory explanations for this discrepancy, one possible reason is that Wnt/β-catenin signaling may not play as important role in OS development as in colon cancer or ovarian cancer. Nonetheless, these results strongly suggest that niclosamide may exert its anticancer activity in OS cells by targeting multiple signaling pathways. Future investigations should be directed to exploring the antitumor activity in animal models of human OS tumors, and ultimately in clinical trials.

## CONCLUSIONS

In summary, we find that niclosamide can effectively inhibit OS cell proliferation and survival, as well as cell migration and wounding closure. Niclosamide is capable of inducing cell apoptosis and inhibits cell cycle progression in OS cells. We further analyze the niclosamide's effect on 11 cancer-related signal pathway reporters and find that three of the tested 11 pathway reporters, E2F1, AP1, and c-Myc-responsive reporters, are significantly inhibited at as early as 24h after niclosamide treatment. The E2F1 and AP1 reporters are even more pronouncedly inhibited, while the NFAT and Wnt/β-catenin reporters are not significantly affected by niclosamide treatment. Furthermore, we demonstrate that the expression of c-Fos, c-Jun, E2F1, and c-Myc in OS cells is effectively inhibited by niclosamide. Furthermore, niclosamide exhibits significantly inhibitory effect on tumor growth in the mouse xenograft model of human osteosarcoma cells. Thus, these results strongly suggest that niclosamide may exert its anticancer activity in OS cells by targeting multiple signaling pathways. Future investigations should be directed to exploring the antitumor activity in animal models of human OS tumors, and ultimately in clinical trials.

## CONFLICT OF INTEREST

The author(s) confirm that this article content has no conflict of interest.

## ACKNOWLEDGEMENTS

The reported work was supported in part by research grants from the National Institutes of Health (AT004418, AR50142, AR054381 to TCH, RCH and HHL), and the 973 Program of Ministry of Science and Technology (MOST) of China (#2011CB707900 to TCH). This work was also supported in part by The University of Chicago Core Facility Subsidy grant from the National Center for Advancing Translational Sciences (NCATS) of the National Institutes of Health through Grant UL1 TR000430.

## REFERENCES

[1] Sandberg, A. A.; Bridge, J. A. Updates on the cytogenetics and molecular genetics of bone and soft tissue tumors: osteosarcoma and related tumors. *Cancer Genet Cytogenet* **2003**, *145*, 1-30.

[2] Helman, L. J.; Meltzer, P. Mechanisms of sarcoma development. *Nat Rev Cancer* **2003**, *3*, 685-694.

[3] Haydon, R. C.; Luu, H. H.; He, T. C. Osteosarcoma and osteoblastic differentiation: a new perspective on oncogenesis. *Clin Orthop Relat Res* **2007**, *454*, 237-246.

[4] Tang, N.; Song, W. X.; Luo, J.; Haydon, R. C.; He, T. C. Osteosarcoma development and stem cell differentiation. *Clin Orthop Relat Res* **2008**, *466*, 2114-2130.

[5] Wagner, E. R.; Luther, G.; Zhu, G.; Luo, Q.; Shi, Q.; Kim, S. H.; Gao, J. L.; Huang, E.; Gao, Y.; Yang, K.; Wang, L.; Teven, C.; Luo, X.; Liu, X.; Li, M.; Hu, N.; Su, Y.; Bi, Y.; He, B. C.; Tang, N.; Luo, J.; Chen, L.; Zuo, G.; Rames, R.; Haydon, R. C.; Luu, H. H.; He, T. C. Defective osteogenic differentiation in the development of osteosarcoma. *Sarcoma* **2011**, *2011*, 325238.

[6] Marina, N.; Gebhardt, M.; Teot, L.; Gorlick, R. Biology and therapeutic advances for pediatric osteosarcoma. *Oncologist* **2004**, *9*, 422-441.

[7] Bruland, O. S.; Pihl, A. On the current management of osteosarcoma. A critical evaluation and a proposal for a modified treatment strategy. *Eur J Cancer* **1997**, *33*, 1725-1731.

[8] Gorlick, R.; Anderson, P.; Andrulis, I.; Arndt, C.; Beardsley, G. P.; Bernstein, M.; Bridge, J.; Cheung, N. K.; Dome, J. S.; Ebb, D.; Gardner, T.; Gebhardt, M.; Grier, H.; Hansen, M.; Healey, J.; Helman, L.; Hock, J.; Houghton, J.; Houghton, P.; Huvos, A.; Khanna, C.; Kieran, M.; Kleinerman, E.; Ladanyi, M.; Lau, C.; Malkin, D.; Marina, N.; Meltzer, P.; Meyers, P.; Schofield, D.; Schwartz, C.; Smith, M. A.; Toretsky, J.; Tsokos, M.; Wexler, L.; Wigginton, J.; Withrow, S.; Schoenfeldt, M.; Anderson, B. Biology of childhood osteogenic sarcoma and potential targets for therapeutic development: meeting summary. *Clin Cancer Res* **2003**, *9*, 5442-5453.

[9] Meyers, P. A.; Gorlick, R. Osteosarcoma. *Pediatr Clin North Am* **1997**, *44*, 973-989.

[10] Denduluri, S. K.; Olumuyiwa Idowu, O.; Wang, Z.; Liao, Z.; Yan, Z.; Mohammed, M. K.; Ye, J.; Wei, Q.; Wang, J.; Zhao, L.; Luu, H. H. Insulin-like growth factor (IGF) signaling in tumorigenesis and the development of cancer drug resistance. *Genes Dis* **2015**, *2*, 13-25.

[11] Haydon, R. C.; Deyrup, A.; Ishikawa, A.; Heck, R.; Jiang, W.; Zhou, L.; Feng, T.; King, D.; Cheng, H.; Breyer, B.; Peabody, T.; Simon, M. A.; Montag, A. G.; He, T. C. Cytoplasmic and/or nuclear accumulation of the beta-catenin protein is a frequent event in human osteosarcoma. *Int J Cancer* **2002**, *102*, 338-342.

[12] Luo, J.; Chen, J.; Deng, Z. L.; Luo, X.; Song, W. X.; Sharff, K. A.; Tang, N.; Haydon, R. C.; Luu, H. H.; He, T. C. Wnt signaling and human diseases: what are the therapeutic implications? *Lab Invest* **2007**, *87*, 97-103.

[13] Luo, X.; Sharff, K. A.; Chen, J.; He, T. C.; Luu, H. H. S100A6 expression and function in human osteosarcoma. *Clin Orthop Relat Res* **2008**, *466*, 2060-2070.

[14] Luu, H. H.; Zhang, R.; Haydon, R. C.; Rayburn, E.; Kang, Q.; Si, W.; Park, J. K.; Wang, H.; Peng, Y.; Jiang, W.; He, T. C. Wnt/beta-catenin signaling pathway as a novel cancer drug target. *Curr Cancer Drug Targets* **2004**, *4*, 653-671.

[15] Luu, H. H.; Zhou, L.; Haydon, R. C.; Deyrup, A. T.; Montag, A. G.; Huo, D.; Heck, R.; Heizmann, C. W.; Peabody, T. D.; Simon, M. A.; He, T. C. Increased expression of S100A6 is associated with decreased metastasis and inhibition of cell migration and anchorage independent growth in human osteosarcoma. *Cancer Lett* **2005**, *229*, 135-148.

[16] Rastegar, F.; Gao, J. L.; Shenaq, D.; Luo, Q.; Shi, Q.; Kim, S. H.; Jiang, W.; Wagner, E. R.; Huang, E.; Gao, Y.; Shen, J.; Yang, K.; He, B. C.; Chen, L.; Zuo, G. W.; Luo, J.; Luo, X.; Bi, Y.; Liu, X.; Li, M.; Hu, N.; Wang, L.; Luther, G.; Luu, H. H.; Haydon, R. C.; He, T. C. Lysophosphatidic acid acyltransferase beta (LPAATbeta) promotes the tumor growth of human osteosarcoma. *PLoS One* **2010**, *5*, e14182.

[17] Su, Y.; Wagner, E. R.; Luo, Q.; Huang, J.; Chen, L.; He, B. C.; Zuo, G. W.; Shi, Q.; Zhang, B. Q.; Zhu, G.; Bi, Y.; Luo, J.; Luo, X.; Kim, S. H.; Shen, J.; Rastegar, F.; Huang, E.; Gao, Y.; Gao, J. L.; Yang, K.; Wietholt, C.; Li, M.; Qin, J.; Haydon, R. C.; He, T. C.; Luu, H. H. Insulin-like growth factor binding protein 5 suppresses tumor growth and metastasis of human osteosarcoma. *Oncogene* **2011**, *30*, 3907-3917.

[18] Luther, G. A.; Lamplot, J.; Chen, X.; Rames, R.; Wagner, E. R.; Liu, X.; Parekh, A.; Huang, E.; Kim, S. H.; Shen, J.; Haydon, R. C.; He, T. C.; Luu, H. H. IGFBP5 Domains Exert Distinct Inhibitory Effects on the Tumorigenicity and Metastasis of Human Osteosarcoma. *Cancer Lett* **2013**, *336*, 222-230.

[19] Luo, X.; Chen, J.; Song, W. X.; Tang, N.; Luo, J.; Deng, Z. L.; Sharff, K. A.; He, G.; Bi, Y.; He, B. C.; Bennett, E.; Huang, J.;

Kang, Q.; Jiang, W.; Su, Y.; Zhu, G. H.; Yin, H.; He, Y.; Wang, Y.; Souris, J. S.; Chen, L.; Zuo, G. W.; Montag, A. G.; Reid, R. R.; Haydon, R. C.; Luu, H. H.; He, T. C. Osteogenic BMPs promote tumor growth of human osteosarcomas that harbor differentiation defects. *Lab Invest* **2008**, *88*, 1264-1277.

[20] Luther, G.; Wagner, E. R.; Zhu, G.; Kang, Q.; Luo, Q.; Lamplot, J.; Bi, Y.; Luo, X.; Luo, J.; Teven, C.; Shi, Q.; Kim, S. H.; Gao, J. L.; Huang, E.; Yang, K.; Rames, R.; Liu, X.; Li, M.; Hu, N.; Liu, H.; Su, Y.; Chen, L.; He, B. C.; Zuo, G. W.; Deng, Z. L.; Reid, R. R.; Luu, H. H.; Haydon, R. C.; He, T. C. BMP-9 Induced Osteogenic Differentiation of Mesenchymal Stem Cells: Molecular Mechanism and Therapeutic Potential. *Curr Gene Ther* **2011**, *11*, 229-240.

[21] Wang, J.; Zhang, H.; Zhang, W.; Huang, E.; Wang, N.; Wu, N.; Wen, S.; Chen, X.; Liao, Z.; Deng, F.; Yin, L.; Zhang, J.; Zhang, Q.; Yan, Z.; Liu, W.; Zhang, Z.; Ye, J.; Deng, Y.; Luu, H. H.; Haydon, R. C.; He, T. C.; Deng, F. Bone Morphogenetic Protein-9 (BMP9) Effectively Induces Osteo/Odontoblastic Differentiation of the Reversibly Immortalized Stem Cells of Dental Apical Papilla. *Stem Cells Dev* **2014**, *23*, 1405-1416.

[22] Jo, A.; Denduluri, S. K.; Zhang, B.; Wang, Z.; Yin, L.; Yan, Z.; Kang, R.; Shi, L. L.; Mok, J.; Lee, M. J.; Haydon, R. C. The Versatile Functions of Sox9 in Development, Stem Cells, and Human Diseases. *Genes Dis* **2014**, *1*, 149-161.

[23] Wang, R. N.; Green, J.; Wang, Z.; Deng, Y.; Qiao, M.; Peabody, M.; Zhang, Q.; Ye, J.; Yan, Z.; Denduluri, S.; Idowu, O.; Li, M.; Shen, C.; Hu, A.; Haydon, R. C.; Kang, R.; Mok, J.; Lee, M. J.; Luu, H. L.; Shi, L. L. Bone Morphogenetic Protein (BMP) Signaling in Development and Human Diseases. *Genes Dis* **2014**, *1*, 87-105.

[24] Haydon, R. C.; Zhou, L.; Feng, T.; Breyer, B.; Cheng, H.; Jiang, W.; Ishikawa, A.; Peabody, T.; Montag, A.; Simon, M. A.; He, T. C. Nuclear receptor agonists as potential differentiation therapy agents for human osteosarcoma. *Clin Cancer Res* **2002**, *8*, 1288-1294.

[25] Sell, S. Stem cell origin of cancer and differentiation therapy. *Crit Rev Oncol Hematol* **2004**, *51*, 1-28.

[26] Freemantle, S. J.; Spinella, M. J.; Dmitrovsky, E. Retinoids in cancer therapy and chemoprevention: promise meets resistance. *Oncogene* **2003**, *22*, 7305-7315.

[27] Hansen, L. A.; Sigman, C. C.; Andreola, F.; Ross, S. A.; Kelloff, G. J.; De Luca, L. M. Retinoids in chemoprevention and differentiation therapy. *Carcinogenesis* **2000**, *21*, 1271-1279.

[28] Wagner, E. R.; He, B. C.; Chen, L.; Zuo, G. W.; Zhang, W.; Shi, Q.; Luo, Q.; Luo, X.; Liu, B.; Luo, J.; Rastegar, F.; He, C. J.; Hu, Y.; Boody, B.; Luu, H. H.; He, T. C.; Deng, Z. L.; Haydon, R. C. Therapeutic Implications of PPARgamma in Human Osteosarcoma. *PPAR Res* **2010**, *2010*, 956427.

[29] Mangelsdorf, D. J.; Thummel, C.; Beato, M.; Herrlich, P.; Schutz, G.; Umesono, K.; Blumberg, B.; Kastner, P.; Mark, M.; Chambon, P.; *et al*. The nuclear receptor superfamily: the second decade. *Cell* **1995**, *83*, 835-839.

[30] Park, B. H.; Breyer, B.; He, T. C. Peroxisome proliferator-activated receptors: roles in tumorigenesis and chemoprevention in human cancer. *Curr Opin Oncol* **2001**, *13*, 78-83.

[31] Kersten, S.; Desvergne, B.; Wahli, W. Roles of PPARs in health and disease. *Nature* **2000**, *405*, 421-424.

[32] Murphy, G. J.; Holder, J. C. PPAR-gamma agonists: therapeutic role in diabetes, inflammation and cancer. *Trends Pharmacol Sci* **2000**, *21*, 469-474.

[33] Garattini, E.; Gianni, M.; Terao, M. Retinoid related molecules an emerging class of apoptotic agents with promising therapeutic potential in oncology: pharmacological activity and mechanisms of action. *Curr Pharm Des* **2004**, *10*, 433-448.

[34] He, B. C.; Chen, L.; Zuo, G. W.; Zhang, W.; Bi, Y.; Huang, J.; Wang, Y.; Jiang, W.; Luo, Q.; Shi, Q.; Zhang, B. Q.; Liu, B.; Lei, X.; Luo, J.; Luo, X.; Wagner, E. R.; Kim, S. H.; He, C. J.; Hu, Y.; Shen, J.; Zhou, Q.; Rastegar, F.; Deng, Z. L.; Luu, H. H.; He, T. C.; Haydon, R. C. Synergistic antitumor effect of the activated PPARgamma and retinoid receptors on human osteosarcoma. *Clin Cancer Res* **2010**, *16*, 2235-2245.

[35] Li, Y.; Li, P. K.; Roberts, M. J.; Arend, R. C.; Samant, R. S.; Buchsbaum, D. J. Multi-targeted therapy of cancer by niclosamide: A new application for an old drug. *Cancer Lett* **2014**, *349*, 8-14.

[36] Chen, W.; Chen, M.; Barak, L. S. Development of small molecules targeting the Wnt pathway for the treatment of colon cancer: a high-throughput screening approach. *Am J Physiol Gastrointest Liver Physiol* **2010**, *299*, G293-300.

[37] Osada, T.; Chen, M.; Yang, X. Y.; Spasojevic, I.; Vandeusen, J. B.; Hsu, D.; Clary, B. M.; Clay, T. M.; Chen, W.; Morse, M. A.; Lyerly, H. K. Antihelminth compound niclosamide downregulates Wnt signaling and elicits antitumor responses in tumors with activating APC mutations. *Cancer Res* **2011**, *71*, 4172-4182.

[38] Sack, U.; Walther, W.; Scudiero, D.; Selby, M.; Kobelt, D.; Lemm, M.; Fichtner, I.; Schlag, P. M.; Shoemaker, R. H.; Stein, U. Novel effect of antihelminthic Niclosamide on S100A4-mediated metastatic progression in colon cancer. *J Natl Cancer Inst* **2011**, *103*, 1018-1036.

[39] Li, R.; Hu, Z.; Sun, S. Y.; Chen, Z. G.; Owonikoko, T. K.; Sica, G. L.; Ramalingam, S. S.; Curran, W. J.; Khuri, F. R.; Deng, X. Niclosamide overcomes acquired resistance to erlotinib through suppression of STAT3 in non-small cell lung cancer. *Mol Cancer Ther* **2013**, *12*, 2200-2212.

[40] You, S.; Li, R.; Park, D.; Xie, M.; Sica, G. L.; Cao, Y.; Xiao, Z. Q.; Deng, X. Disruption of STAT3 by niclosamide reverses radioresistance of human lung cancer. *Mol Cancer Ther* **2014**, *13*, 606-616.

[41] Lu, W.; Lin, C.; Roberts, M. J.; Waud, W. R.; Piazza, G. A.; Li, Y. Niclosamide suppresses cancer cell growth by inducing Wnt co-receptor LRP6 degradation and inhibiting the Wnt/beta-catenin pathway. *PLoS One* **2011**, *6*, e29290.

[42] Wang, Y. C.; Chao, T. K.; Chang, C. C.; Yo, Y. T.; Yu, M. H.; Lai, H. C. Drug screening identifies niclosamide as an inhibitor of breast cancer stem-like cells. *PLoS One* **2013**, *8*, e74538.

[43] Ye, T.; Xiong, Y.; Yan, Y.; Xia, Y.; Song, X.; Liu, L.; Li, D.; Wang, N.; Zhang, L.; Zhu, Y.; Zeng, J.; Wei, Y.; Yu, L. The anthelmintic drug niclosamide induces apoptosis, impairs metastasis and reduces immunosuppressive cells in breast cancer model. *PLoS One* **2014**, *9*, e85887.

[44] Londono-Joshi, A. I.; Arend, R. C.; Aristizabal, L.; Lu, W.; Samant, R. S.; Metge, B. J.; Hidalgo, B.; Grizzle, W. E.; Conner, M.; Forero-Torres, A.; Lobuglio, A. F.; Li, Y.; Buchsbaum, D. J. Effect of niclosamide on basal-like breast cancers. *Mol Cancer Ther* **2014**, *13*, 800-811.

[45] Yo, Y. T.; Lin, Y. W.; Wang, Y. C.; Balch, C.; Huang, R. L.; Chan, M. W.; Sytwu, H. K.; Chen, C. K.; Chang, C. C.; Nephew, K. P.; Huang, T.; Yu, M. H.; Lai, H. C. Growth inhibition of ovarian tumor-initiating cells by niclosamide. *Mol Cancer Ther* **2012**, *11*, 1703-1712.

[46] King, M. L.; Lindberg, M. E.; Stodden, G. R.; Okuda, H.; Ebers, S. D.; Johnson, A.; Montag, A.; Lengyel, E.; MacLean Ii, J. A.; Hayashi, K. WNT7A/beta-catenin signaling induces FGF1 and influences sensitivity to niclosamide in ovarian cancer. *Oncogene* **2014**.

[47] Arend, R. C.; Londono-Joshi, A. I.; Samant, R. S.; Li, Y.; Conner, M.; Hidalgo, B.; Alvarez, R. D.; Landen, C. N.; Straughn, J. M.; Buchsbaum, D. J. Inhibition of Wnt/beta-catenin pathway by niclosamide: a therapeutic target for ovarian cancer. *Gynecol Oncol* **2014**, *134*, 112-120.

[48] Liu, C.; Lou, W.; Zhu, Y.; Nadiminty, N.; Schwartz, C. T.; Evans, C. P.; Gao, A. C. Niclosamide inhibits androgen receptor variants expression and overcomes enzalutamide resistance in castration-resistant prostate cancer. *Clin Cancer Res* **2014**, *20*, 3198-3210.

[49] Wieland, A.; Trageser, D.; Gogolok, S.; Reinartz, R.; Hofer, H.; Keller, M.; Leinhaas, A.; Schelle, R.; Normann, S.; Klaas, L.; Waha, A.; Koch, P.; Fimmers, R.; Pietsch, T.; Yachnis, A. T.; Pincus, D. W.; Steindler, D. A.; Brustle, O.; Simon, M.; Glas, M.; Scheffler, B. Anticancer effects of niclosamide in human glioblastoma. *Clin Cancer Res* **2013**, *19*, 4124-4136.

[50] Li, R.; You, S.; Hu, Z.; Chen, Z. G.; Sica, G. L.; Khuri, F. R.; Curran, W. J.; Shin, D. M.; Deng, X. Inhibition of STAT3 by niclosamide synergizes with erlotinib against head and neck cancer. *PLoS One* **2013**, *8*, e74670.

[51] Wang, A. M.; Ku, H. H.; Liang, Y. C.; Chen, Y. C.; Hwu, Y. M.; Yeh, T. S. The autonomous notch signal pathway is activated by baicalin and baicalein but is suppressed by niclosamide in K562 cells. *J Cell Biochem* **2009**, *106*, 682-692.

[52] Jin, Y.; Lu, Z.; Ding, K.; Li, J.; Du, X.; Chen, C.; Sun, X.; Wu, Y.; Zhou, J.; Pan, J. Antineoplastic mechanisms of niclosamide in acute myelogenous leukemia stem cells: inactivation of the NF-kappaB pathway and generation of reactive oxygen species. *Cancer Res* **2010**, *70*, 2516-2527.

[53] Ono, M.; Yin, P.; Navarro, A.; Moravek, M. B.; Coon, V. J.; Druschitz, S. A.; Gottardi, C. J.; Bulun, S. E. Inhibition of

canonical WNT signaling attenuates human leiomyoma cell growth. *Fertil Steril* **2014**, *101*, 1441-1449.

[54] Mook, R. A., Jr.; Chen, M.; Lu, J.; Barak, L. S.; Lyerly, H. K.; Chen, W. Small molecule modulators of Wnt/beta-catenin signaling. *Bioorg Med Chem Lett* **2013**, *23*, 2187-2191.

[55] Wang, N.; Zhang, H.; Zhang, B. Q.; Liu, W.; Zhang, Z.; Qiao, M.; Zhang, H.; Deng, F.; Wu, N.; Chen, X.; Wen, S.; Zhang, J.; Liao, Z.; Zhang, Q.; Yan, Z.; Yin, L.; Ye, J.; Deng, Y.; Luu, H. H.; Haydon, R. C.; Liang, H.; He, T. C. Adenovirus-mediated efficient gene transfer into cultured three-dimensional organoids. *PLoS One* **2014**, *9*, e93608.

[56] Wang, N.; Zhang, W.; Cui, J.; Zhang, H.; Chen, X.; Li, R.; Wu, N.; Chen, X.; Wen, S.; Zhang, J.; Yin, L.; Deng, F.; Liao, Z.; Zhang, Z.; Zhang, Q.; Yan, Z.; Liu, W.; Ye, J.; Deng, Y.; Wang, Z.; Qiao, M.; Luu, H. H.; Haydon, R. C.; Shi, L. L.; Liang, H.; He, T. C. The piggyBac Transposon-Mediated Expression of SV40 T Antigen Efficiently Immortalizes Mouse Embryonic Fibroblasts (MEFs). *PLoS One* **2014**, *9*, e97316.

[57] Lamplot, J. D.; Liu, B.; Yin, L.; Zhang, W.; Wang, Z.; Luther, G.; Wagner, E.; Li, R.; Nan, G.; Shui, W.; Yan, Z.; Rames, R.; Deng, F.; Zhang, H.; Liao, Z.; Liu, W.; Zhang, J.; Zhang, Z.; Zhang, Q.; Ye, J.; Deng, Y.; Qiao, M.; Haydon, R. C.; Luu, H. H.; Angeles, J.; Shi, L. L.; He, T. C.; Ho, S. H. Reversibly Immortalized Mouse Articular Chondrocytes Acquire Long-Term Proliferative Capability while Retaining Chondrogenic Phenotype. *Cell Transplant* **2015**.

[58] Wen, S.; Zhang, H.; Li, Y.; Wang, N.; Zhang, W.; Yang, K.; Wu, N.; Chen, X.; Deng, F.; Liao, Z.; Zhang, J.; Zhang, Q.; Yan, Z.; Liu, W.; Zhang, Z.; Ye, J.; Deng, Y.; Zhou, G.; Luu, H. H.; Haydon, R. C.; Shi, L. L.; He, T. C.; Wei, G. Characterization of constitutive promoters for piggyBac transposon-mediated stable transgene expression in mesenchymal stem cells (MSCs). *PLoS One* **2014**, *9*, e94397.

[59] Zhao, C.; Wu, N.; Deng, F.; Zhang, H.; Wang, N.; Zhang, W.; Chen, X.; Wen, S.; Zhang, J.; Yin, L.; Liao, Z.; Zhang, Z.; Zhang, Q.; Yan, Z.; Liu, W.; Wu, D.; Ye, J.; Deng, Y.; Zhou, G.; Luu, H. H.; Haydon, R. C.; Si, W.; He, T. C. Adenovirus-mediated gene transfer in mesenchymal stem cells can be significantly enhanced by the cationic polymer polybrene. *PLoS One* **2014**, *9*, e92908.

[60] Li, R.; Zhang, W.; Cui, J.; Shui, W.; Yin, L.; Wang, Y.; Zhang, H.; Wang, N.; Wu, N.; Nan, G.; Chen, X.; Wen, S.; Deng, F.; Zhang, H.; Zhou, G.; Liao, Z.; Zhang, J.; Zhang, Q.; Yan, Z.; Liu, W.; Zhang, Z.; Ye, J.; Deng, Y.; Luu, H. H.; Haydon, R. C.; He, T. C.; Deng, Z. L. Targeting BMP9-Promoted Human Osteosarcoma Growth by Inactivation of Notch Signaling. *Curr Cancer Drug Targets* **2014**.

[61] Chen, X.; Cui, J.; Yan, Z.; Zhang, H.; Chen, X.; Wang, N.; Shah, P.; Deng, F.; Zhao, C.; Geng, N.; Li, M.; Denduluri, S. K.; Haydon, R. C.; Luu, H. H.; Reid, R. R.; He, T. C. Sustained high level transgene expression in mammalian cells mediated by the optimized piggyBac transposon system. *Genes Dis* **2015**, *2*, 96-105.

[62] Luu, H. H.; Kang, Q.; Park, J. K.; Si, W.; Luo, Q.; Jiang, W.; Yin, H.; Montag, A. G.; Simon, M. A.; Peabody, T. D.; Haydon, R. C.; Rinker-Schaeffer, C. W.; He, T. C. An orthotopic model of human osteosarcoma growth and spontaneous pulmonary metastasis. *Clin Exp Metastasis* **2005**, *22*, 319-329.

[63] Luo, Q.; Kang, Q.; Si, W.; Jiang, W.; Park, J. K.; Peng, Y.; Li, X.; Luu, H. H.; Luo, J.; Montag, A. G.; Haydon, R. C.; He, T. C. Connective Tissue Growth Factor (CTGF) Is Regulated by Wnt and Bone Morphogenetic Proteins Signaling in Osteoblast Differentiation of Mesenchymal Stem Cells. *J Biol Chem* **2004**, *279*, 55958-55968.

[64] Si, W.; Kang, Q.; Luu, H. H.; Park, J. K.; Luo, Q.; Song, W. X.; Jiang, W.; Luo, X.; Li, X.; Yin, H.; Montag, A. G.; Haydon, R. C.; He, T. C. CCN1/Cyr61 Is Regulated by the Canonical Wnt Signal and Plays an Important Role in Wnt3A-Induced Osteoblast Differentiation of Mesenchymal Stem Cells. *Mol Cell Biol* **2006**, *26*, 2955-2964.

[65] Su, Y.; Luo, X.; He, B. C.; Wang, Y.; Chen, L.; Zuo, G. W.; Liu, B.; Bi, Y.; Huang, J.; Zhu, G. H.; He, Y.; Kang, Q.; Luo, J.; Shen, J.; Chen, J.; Jin, X.; Haydon, R. C.; He, T. C.; Luu, H. H. Establishment and characterization of a new highly metastatic human osteosarcoma cell line. *Clin Exp Metastasis* **2009**, *26*, 599-610.

[66] He, B. C.; Gao, J. L.; Zhang, B. Q.; Luo, Q.; Shi, Q.; Kim, S. H.; Huang, E.; Gao, Y.; Yang, K.; Wagner, E. R.; Wang, L.; Tang, N.; Luo, J.; Liu, X.; Li, M.; Bi, Y.; Shen, J.; Luther, G.; Hu, N.; Zhou, Q.; Luu, H. H.; Haydon, R. C.; Zhao, Y.; He, T. C. Tetrandrine inhibits Wnt/beta-catenin signaling and suppresses tumor growth of human colorectal cancer. *Mol Pharmacol* **2011**, *79*, 211-219.

[67] He, B. C.; Gao, J. L.; Luo, X.; Luo, J.; Shen, J.; Wang, L.; Zhou, Q.; Wang, Y. T.; Luu, H. H.; Haydon, R. C.; Wang, C. Z.; Du, W.; Yuan, C. S.; He, T. C.; Zhang, B. Q. Ginsenoside Rg3 inhibits colorectal tumor growth through the down-regulation of Wnt/ss-catenin signaling. *Int J Oncol* **2011**, *38*, 437-445.

[68] Zhang, Y.; Chen, X.; Qiao, M.; Zhang, B. Q.; Wang, N.; Zhang, Z.; Liao, Z.; Zeng, L.; Deng, Y.; Deng, F.; Zhang, J.; Yin, L.; Liu, W.; Zhang, Q.; Ya, Z.; Ye, J.; Wang, Z.; Zhou, L.; Luu, H. H.; Haydon, R. C.; He, T. C.; Zhang, H. Bone morphogenetic protein 2 inhibits the proliferation and growth of human colorectal cancer cells. *Oncol Rep* **2014**.

[69] Zhu, G. H.; Huang, J.; Bi, Y.; Su, Y.; Tang, Y.; He, B. C.; He, Y.; Luo, J.; Wang, Y.; Chen, L.; Zuo, G. W.; Jiang, W.; Luo, Q.; Shen, J.; Liu, B.; Zhang, W. L.; Shi, Q.; Zhang, B. Q.; Kang, Q.; Zhu, J.; Tian, J.; Luu, H. H.; Haydon, R. C.; Chen, Y.; He, T. C. Activation of RXR and RAR signaling promotes myogenic differentiation of myoblastic C2C12 cells. *Differentiation* **2009**, *78* 195–204.

[70] Li, M.; Chen, Y.; Bi, Y.; Jiang, W.; Luo, Q.; He, Y.; Su, Y.; Liu, X.; Cui, J.; Zhang, W.; Li, R.; Kong, Y.; Zhang, J.; Wang, J.; Zhang, H.; Shui, W.; Wu, N.; Zhu, J.; Tian, J.; Yi, Q. J.; Luu, H. H.; Haydon, R. C.; He, T. C.; Zhu, G. H. Establishment and characterization of the reversibly immortalized mouse fetal heart progenitors. *Int J Med Sci* **2013**, *10*, 1035-1046.

[71] Zhang, H.; Wang, J.; Deng, F.; Huang, E.; Yan, Z.; Wang, Z.; Deng, Y.; Zhang, Q.; Zhang, Z.; Ye, J.; Qiao, M.; Li, R.; Wang, J.; Wei, Q.; Zhou, G.; Luu, H. H.; Haydon, R. C.; He, T. C.; Deng, F. Canonical Wnt signaling acts synergistically on BMP9-induced osteo/odontoblastic differentiation of stem cells of dental apical papilla (SCAPs). *Biomaterials* **2015**, *39*, 145-154.

[72] Gao, J. L.; Lv, G. Y.; He, B. C.; Zhang, B. Q.; Zhang, H.; Wang, N.; Wang, C. Z.; Du, W.; Yuan, C. S.; He, T. C. Ginseng saponin metabolite 20(S)-protopanaxadiol inhibits tumor growth by targeting multiple cancer signaling pathways. *Oncol Rep* **2013**, *30*, 292-298.

[73] Huang, J.; Bi, Y.; Zhu, G. H.; He, Y.; Su, Y.; He, B. C.; Wang, Y.; Kang, Q.; Chen, L.; Zuo, G. W.; Luo, Q.; Shi, Q.; Zhang, B. Q.; Huang, A.; Zhou, L.; Feng, T.; Luu, H. H.; Haydon, R. C.; He, T. C.; Tang, N. Retinoic acid signalling induces the differentiation of mouse fetal liver-derived hepatic progenitor cells. *Liver Int* **2009**, *29*, 1569-1581.

[74] Zhang, W.; Deng, Z. L.; Chen, L.; Zuo, G. W.; Luo, Q.; Shi, Q.; Zhang, B. Q.; Wagner, E. R.; Rastegar, F.; Kim, S. H.; Jiang, W.; Shen, J.; Huang, E.; Gao, Y.; Gao, J. L.; Zhou, J. Z.; Luo, J.; Huang, J.; Luo, X.; Bi, Y.; Su, Y.; Yang, K.; Liu, H.; Luu, H. H.; Haydon, R. C.; He, T. C.; He, B. C. Retinoic acids potentiate BMP9-induced osteogenic differentiation of mesenchymal progenitor cells. *PLoS One* **2010**, *5*, e11917.

[75] Huang, E.; Zhu, G.; Jiang, W.; Yang, K.; Gao, Y.; Luo, Q.; Gao, J. L.; Kim, S. H.; Liu, X.; Li, M.; Shi, Q.; Hu, N.; Wang, L.; Liu, H.; Cui, J.; Zhang, W.; Li, R.; Chen, X.; Kong, Y. H.; Zhang, J.; Wang, J.; Shen, J.; Bi, Y.; Statz, J.; He, B. C.; Luo, J.; Wang, H.; Xiong, F.; Luu, H. H.; Haydon, R. C.; Yang, L.; He, T. C. Growth hormone synergizes with BMP9 in osteogenic differentiation by activating the JAK/STAT/IGF1 pathway in murine multilineage cells. *J Bone Miner Res* **2012**, *27*, 1566-1575.

[76] Sharff, K. A.; Song, W. X.; Luo, X.; Tang, N.; Luo, J.; Chen, J.; Bi, Y.; He, B. C.; Huang, J.; Li, X.; Jiang, W.; Zhu, G. H.; Su, Y.; He, Y.; Shen, J.; Wang, Y.; Chen, L.; Zuo, G. W.; Liu, B.; Pan, X.; Reid, R. R.; Luu, H. H.; Haydon, R. C.; He, T. C. Hey1 Basic Helix-Loop-Helix Protein Plays an Important Role in Mediating BMP9-induced Osteogenic Differentiation of Mesenchymal Progenitor Cells. *J Biol Chem* **2009**, *284*, 649-659.

[77] Hu, N.; Jiang, D.; Huang, E.; Liu, X.; Li, R.; Liang, X.; Kim, S. H.; Chen, X.; Gao, J. L.; Zhang, H.; Zhang, W.; Kong, Y. H.; Zhang, J.; Wang, J.; Shui, W.; Luo, X.; Liu, B.; Cui, J.; Rogers, M. R.; Shen, J.; Zhao, C.; Wang, N.; Wu, N.; Luu, H. H.; Haydon, R. C.; He, T. C.; Huang, W. BMP9-regulated angiogenic signaling plays an important role in the osteogenic differentiation of mesenchymal progenitor cells. *J Cell Sci* **2013**, *126*, 532-541.

[78] Huang, E.; Bi, Y.; Jiang, W.; Luo, X.; Yang, K.; Gao, J. L.; Gao, Y.; Luo, Q.; Shi, Q.; Kim, S. H.; Liu, X.; Li, M.; Hu, N.; Liu, H.; Cui, J.; Zhang, W.; Li, R.; Chen, X.; Shen, J.; Kong, Y.; Zhang, J.; Wang, J.; Luo, J.; He, B. C.; Wang, H.; Reid, R. R.; Luu, H. H.;

Haydon, R. C.; Yang, L.; He, T. C. Conditionally Immortalized Mouse Embryonic Fibroblasts Retain Proliferative Activity without Compromising Multipotent Differentiation Potential. *PLoS One* **2012**, *7*, e32428.

[79] Wu, N.; Zhang, H.; Deng, F.; Li, R.; Zhang, W.; Chen, X.; Wen, S.; Wang, N.; Zhang, J.; Yin, L.; Liao, Z.; Zhang, Z.; Zhang, Q.; Yan, Z.; Liu, W.; Wu, D.; Ye, J.; Deng, Y.; Yang, K.; Luu, H. H.; Haydon, R. C.; He, T. C. Overexpression of Ad5 precursor terminal protein accelerates recombinant adenovirus packaging and amplification in HEK-293 packaging cells. *Gene Ther* **2014**, *21*, 629-637.

[80] Deng, F.; Chen, X.; Liao, Z.; Yan, Z.; Wang, Z.; Deng, Y.; Zhang, Q.; Zhang, Z.; Ye, J.; Qiao, M.; Li, R.; Denduluri, S.; Wang, J.; Wei, Q.; Li, M.; Geng, N.; Zhao, L.; Zhou, G.; Zhang, P.; Luu, H. H.; Haydon, R. C.; Reid, R. R.; Yang, T.; He, T. C. A Simplified and Versatile System for the Simultaneous Expression of Multiple siRNAs in Mammalian Cells Using Gibson DNA Assembly. *PLoS One* **2014**, *9*, e113064.

[81] Bi, Y.; He, Y.; Huang, J.; Su, Y.; Zhu, G. H.; Wang, Y.; Qiao, M.; Zhang, B. Q.; Zhang, H.; Wang, Z.; Liu, W.; Cui, J.; Kang, Q.; Zhang, Z.; Deng, Y.; Li, R.; Zhang, Q.; Yang, K.; Luu, H. H.; Haydon, R. C.; He, T. C.; Tang, N. Functional characteristics of reversibly immortalized hepatic progenitor cells derived from mouse embryonic liver. *Cell Physiol Biochem* **2014**, *34*, 1318-1338.

[82] Balgi, A. D.; Fonseca, B. D.; Donohue, E.; Tsang, T. C.; Lajoie, P.; Proud, C. G.; Nabi, I. R.; Roberge, M. Screen for chemical modulators of autophagy reveals novel therapeutic inhibitors of mTORC1 signaling. *PLoS One* **2009**, *4*, e7124.

[83] Fonseca, B. D.; Diering, G. H.; Bidinosti, M. A.; Dalal, K.; Alain, T.; Balgi, A. D.; Forestieri, R.; Nodwell, M.; Rajadurai, C. V.; Gunaratnam, C.; Tee, A. R.; Duong, F.; Andersen, R. J.; Orlowski, J.; Numata, M.; Sonenberg, N.; Roberge, M. Structure-activity analysis of niclosamide reveals potential role for cytoplasmic pH in control of mammalian target of rapamycin complex 1 (mTORC1) signaling. *J Biol Chem* **2012**, *287*, 17530-17545.

[84] Ren, X.; Duan, L.; He, Q.; Zhang, Z.; Zhou, Y.; Wu, D.; Pan, J.; Pei, D.; Ding, K. Identification of Niclosamide as a New Small-Molecule Inhibitor of the STAT3 Signaling Pathway. *ACS Med Chem Lett* **2010**, *1*, 454-459.

[85] Li, Z.; Yu, Y.; Sun, S.; Qi, B.; Wang, W.; Yu, A. Niclosamide inhibits the proliferation of human osteosarcoma cell lines by inducing apoptosis and cell cycle arrest. *Oncol Rep* **2015**, *33*, 1763-1768.

[86] Lee, S. L.; Son, A. R.; Ahn, J.; Song, J. Y. Niclosamide enhances ROS-mediated cell death through c-Jun activation. *Biomed Pharmacother* **2014**, *68*, 619-624.